

# A Case Study of Wood Thermoplastic Composite Filament for 3D Printing

Veysel Tokdemir <sup>a,\*</sup> and Suat Altun <sup>b</sup>

The 3D printing technology is a method of converting proposed complex geometric shapes into solid models. One of these methods is the FDM (fused deposition modeling) printing technology as a considerably affordable and the most commonly used method in the world. The purpose of this study is to obtain FDM 3D printer filaments that are as natural as possible, resembling wood and evoking the sensation of wood upon touching through deployment of bio-based plastics and additives. Polylactic acid (PLA) and bio thermoplastic polyurethane (TPU) were used as matrices, and lignin and Arboform, a lignin-based biomaterial, were used as additives. The characteristics of composites achieved through addition of 10% lignin and Arboform to matrices were identified by differential scanning calorimetry (DSC) thermogravimetric analysis (TGA), scanning electron microscopy (SEM), and the tensile test. The effects of some printing parameters on the mechanical characteristics were also determined. Lignin induced a decrease in mechanical characteristics for both PLA and TPU. Arboform, on the other hand, demonstrated good bonding with TPU and increased tensile strength. Production of flexible and sufficiently durable parts by means of 10% Arboform-containing TPU filaments was demonstrated.

DOI: 10.15376/biores.17.1.21-36

Keywords: Bio-based wood filaments; TPU; PLA; Lignin; Arboform; 3D printing

Contact information: a: Department of Interior Design Safranbolu Vocational School, Karabuk University, Safranbolu/Karabuk, Turkey; b: Department of Industrial Design Engineering, Karabuk University, Karabuk, Turkey; \*Corresponding author: veyseltokdemir@karabuk.edu.tr

## INTRODUCTION

People's interest in 3D printing has been increasing in the recent years. Fused deposition modeling (FDM), selective laser sintering (SLS), and various similar technologies are used in 3D printing. Amongst such, the FDM technology is the most widely used method on account of both its simple operating logic and its affordability. (Credi *et al.* 2016). Thus, the FDM printing technology is constantly evolving, and the printing materials play a significant role in its sustainable development (Lee *et al.* 2014; Liu *et al.* 2019).

Thermoplastic materials such as polylactic acid (PLA), acrylonitrile butadiene styrene (ABS), polycarbonate (PC), and thermoplastic polyurethane (TPU) are generally used with the FDM technology (Bates *et al.* 2016; Fernandes *et al.* 2018; Raj *et al.* 2018; Nguyen *et al.* 2018). Different materials are preferred according to the purpose and characteristics of the object to be printed. TPU is preferred for its flexible structure, whereas PLA is preferred for being biodegradable and biosourced. However, the use of PLA in 3D printing is limited due to its production cost, brittleness, poor heat resistance,

and tensile properties; likewise TPU has high cost, limited mechanical properties and there are issues encountered during printing (Bates *et al.* 2016; Liu *et al.* 2019).

The development of environmentally friendly and recycled materials has also increased interest in biodegradable 3D printing materials. Addition of natural additives to thermoplastic materials at certain ratios improves mechanical characteristics and enables production of more environmentally friendly materials. Products with improved biodegradability can be achieved by adding waste agricultural products such as wood dust, hemp and flax fiber, or coconut shell to thermoplastics (Mazzanti *et al.* 2019). This includes not only wood, but also cellulose, hemicelluloses, or lignin, which are the building blocks of wood (Wimmer *et al.* 2015). Following cellulose, lignin is the second most naturally occurring biopolymer in abundance in the cell wall (15 to 35%) of lignocellulosic compound. Lignin can be produced in large quantities as a by-product through various processes in biorefineries and in the pulp and paper industries. Most of the lignin is used in generation of energy and is perpetually treated as waste. It is considered a potential material for the production of various polymers, and biomaterials due to the high content of phenolic compounds. Lignin-based copolymers and modified lignin exert favorable miscibility with many polymeric matrices and exhibit superior characteristics (Gordobil *et al.* 2015; Dehne *et al.* 2016; Solihat *et al.* 2021; Spiridon *et al.* 2015; Spiridon and Tanase 2018; Li *et al.* 2020). Blending polymers with lignin is considered to be a convenient and inexpensive method for creating new materials with special abilities such as hydrophobicity, hardness, crystallinity, thermal stability, ultraviolet (UV) blocking ability, and for reducing the overall cost of the material (Gkartzou *et al.* 2017).

Wood-plastic composite material not only combines wood and plastic, but it also makes it possible to achieve advantageous novelty materials by remedying the individual deficiencies of the materials (Afrose *et al.* 2016; Bhattacharjee *et al.* 2016). Scientists have conducted research on improving the performance of PLA-based wood-plastic composites for 3D printing and reported that the type and content of plant fibers in the composites significantly affect wood-plastic performance (Liu *et al.* 2019). Academic studies demonstrated that the addition of lignin at certain ratios reveals high compatibility between PLA and lignin (Gkartzou *et al.* 2017; Mimini *et al.* 2019; Tanase-Opedal *et al.* 2019).

Despite a number of studies on PLA-based materials to be used in FDM being available, only a very few studies on PLA-based bio-composites exist. Although studies in which filaments self-produced by the researchers are used rather than the commercially available filaments have been emerging lately, studies examining the effects of the formulation of additives, filament preparation process and parameters, printing geometry and patterns are limited (Mazzanti *et al.* 2019). PLA-based wood filaments are commercially available, whereas no flexible wood filament is obtainable. Only one scientific study which produced flexible filament with TPU matrix and wood additives has been found (Bi *et al.* 2018). The cited authors stated that there is a good interface bonding of wood flour modified with diphenylmethyl propane diisocyanate (MDI) and EPDM-g-MAH with TPU, and that flat-surface flexible parts can be printed with the produced filament.

The aim of this study is to examine printing parameters and certain characteristics by obtaining FDM printer filaments that are as natural as possible, resembling wood and evoking the sensation of wood upon touching through deployment of bio-based plastics (Mimini *et al.* 2019) and additives. For such purpose, completely biodegradable and biologically sourced PLA and 65% biologically sourced TPU were chosen as the matrices.

Organosolv lignin and lignin-based thermoplastic material, also known as liquid wood, and commercially called Arboform (ARB) were used as wood-derived additives. Some thermal and mechanical characteristics of the resulting composite filament and the effects of printing parameters on the tensile strength were identified.

## EXPERIMENTAL

### Materials

The PLA with the commercial title Purapol LX175, used as a matrix in the study, was procured from Kumru Kimya San. ve Tic. Ltd. Şti. (Istanbul, Turkey). The density of the PLA matrix used is 1240 kg/m<sup>3</sup>, the maximum tensile strength is 45 MPa, and the elongation at break is maximum 5% (<http://www.corbion.com/media/442336/pds-purapol-lx175.pdf>). The other matrix of TPU (Covestro Bio Grade Series: DESMOPAN DP.33085AU DPS300), a polymer produced from 65% bioresources, was procured from Albis Plastik San. ve Tic. Ltd. Şti. (Istanbul, Turkey). The density of this matrix is 1270 kg/m<sup>3</sup>, Shore A hardness (method A) 87, and ultimate tensile strength 42 MPa, as declared by the manufacturer in the material data sheet.

The Lignin (L) which is used as an additive was procured from Lignol Innovations Inc. (Burnaby, Canada). Organosolv lignin extracted from hardwood chips is of dark brown and powdery form. It is a natural and thermoplastic component that is one of the basic building blocks of wood.

The lignin-based thermoplastic material, commercially called Arboform LV4 (ARB), used as an additive material, was procured from Albis Plastik San. Tic. Ltd. Şti. (Istanbul, Turkey) in granular form. Arboform LV4, a 100% renewable and biodegradable material produced from natural fibers and natural additives, is an odorless material with low shrinkage and moderate thermal resistance. Some characteristics of this material has been provided on the material data sheet by the manufacturer as 1270 kg/m<sup>3</sup> of density, 3 kJ/m<sup>2</sup> of notched impact resistance, 27 MPa of stress at break, 0.4 of strain at break, and 28 MPa of tensile strength (Arboform LV4 2021).

### Methods

PLA, TPU, and ARB were procured in granular form, and L was procured in powder form. In order for L mixtures to form homogeneous composites in the melt mixing process, PLA-L and TPU-L groups were mixed as powder, while PLA-ARB and TPU-ARB groups were mixed as granules. Therefore, a proportion of the PLA and TPU was ground into powder by grinding in a plastic grinder (Mipro MLD, Protek Group Lab, Ankara, Turkey) and then sieved with a vibrating sieve (Loyka ESM 200, Akyol Trade Co., Ltd., Istanbul, Turkey) for sizing. (Fig. 1a). The materials remaining in the range of 288 to 666 µm following the sieving process were used in the mixtures.

According to literature, the optimum ratio of wood or derivative additives to be used has been observed to be 10% by weight (Kariz *et al.* 2018; Mimini *et al.* 2019). Thus, the L and ARB additives were added to the matrices at a level of 10% by weight. The materials weighed on precision scales were combined in separate jars for each group. In order to obtain homogeneous mixtures, they were mixed in a multidirectional mechanical powder mixer (Turbula TF2 3D, Basel, Switzerland) (Fig. 1b) for 4 h for powdered groups and for 2 h for granular groups. The resulting mixtures are shown in Fig. 1. The mixed

groups were dried in an oven at 60 °C for 12 h for the removal of the moisture contained prior to composition in a twin-screw extruder.

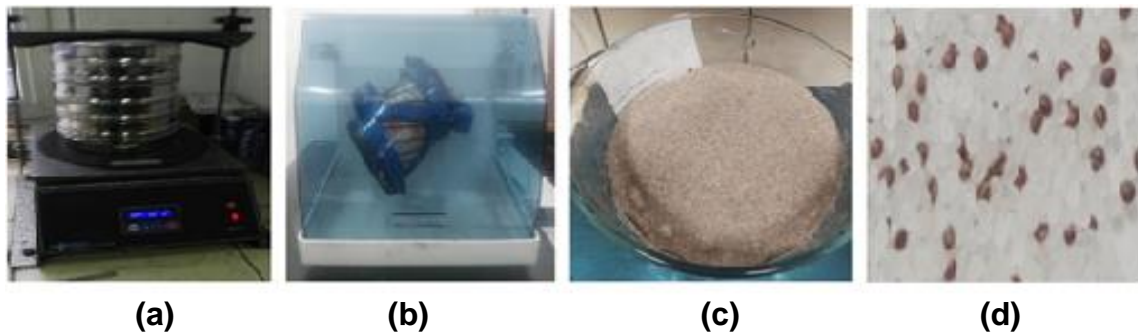


**Fig. 1.** (a) Vibrating sieve, (b) versatile mechanical powder mixer, (c) powder mixture, and (d) granular mixture

### Preparation of Composites

The mixtures dried in the oven were melted and mixed in a twin-screw extruder with a diameter of 18 mm and an  $L/D$  ratio of 44 (Polartek Polymer Research Technologies Ind. Trade Co., Ltd., Istanbul, Turkey). All groups were extruded at a temperature of 190 °C and a feed rate of 15 m/min. Granulated with the help of a crusher, the composites were dried in an oven at 60 °C for 72 h.

### Preparation of Tensile Test Specimens by Injection Molding

Tensile test specimens in accordance with the ASTM D638 Type IV standard were acquired from some of the dried composites via the injection molding method. A total of 30 specimens were prepared for 6 groups with 5 specimens for each group. The injection device consists of 3 heating zones. The feeding zone, which is the first heating zone, was set to 160 °C, whereas the other heating zones were set to 180 °C, and the injection process was carried out at 25 rpm rotating speed of the screw



**Fig. 2.** Single screw extruder

### Production of Filaments

The dried composite granules were transformed into filaments with a diameter of 1.75 mm via a single screw extruder with a diameter of 16 mm, an  $L/D$  ratio of 25, and three heating zones (Polartek Polymer Research Technologies Ind. Trade Co., Ltd.,

Istanbul, Turkey). The temperature settings and feeding speed are of great significance in filament production. Inconsistencies in filament diameters or occurrences of filament breaks and sagging during extrusion are possible. As a result of trial productions using different parameters, the parameters with which the best production were achieved, and the filaments used in the next stages are described in Table 1. Diameter control in filament production was measured by instantaneous reading by sensors, and filaments with a diameter range of 1.65 to 1.85 mm were produced.

**Table 1.** Filament Production Parameters at Single Screw Extruder

Group Name	Temperature (°C)			Feed Rate (rpm)
	1 <sup>st</sup> Zone	2 <sup>nd</sup> Zone	3 <sup>rd</sup> Zone	
PLA	170	175	175	13.7
PLA-L	190	190	190	14.5
PLA-ARB	190	195	195	12.2
TPU	195	200	200	10.4
TPU-L	190	198	198	9.7
TPU-ARB	195	200	200	10.1

\*PLA: Pure PLA, PLA-L: 90% PLA+10% L, PLA-ARB: 90% PLA+10% ARB, TPU: Pure TPU, TPU-L: 90% TPU+10% L, TPU-ARB: 90% TPU+10% ARB

### 3D Printing of Tensile Test Specimens

The tensile strength test was carried out in order to determine the effect of the printing parameters on the mechanical characteristics of the pieces produced with 3D printers with the resulting composite filaments. ASTM D638-14 (2014) type IV tensile test specimens were modeled using Autocad (Student Version, Autodesk, San Rafael, CA, USA) software and saved in stl format. The Simplify 3D (Simplify 3D, Cincinnati, USA) software was utilized to generate G codes, layer and edit printing parameters. The FDM printer (Xperia, Yapılcı Machine Ind. Trade. Co., Ltd., Corum, Turkey) and 0.6 mm diameter nozzles were used for printing of 5 specimens for each group (Fig. 3).

Beside the availability of many different printing parameters, the most important factor affecting the mechanical characteristics of a 3D printed piece is the bonding between the printing layers. The most tested printing factors for pieces printed with natural fiber reinforced filaments are nozzle diameter, printing temperature, bearing temperature, printing speed, and layer thickness (Mazzanti *et al.* 2019). The parameters such as nozzle diameter, layer thickness, infill geometry, and infill rate exhibit similar effects for all filaments. However, the foremost factors affecting the bonding between filament layers are printing temperature and printing speed. Experiments were conducted in this regard at many different printing speeds and temperatures, and only the results of the parameters which can be successfully printed are given in this article. Since the 3D printer extruder heating tolerance is  $\pm 5$  °C, a temperature difference of at least 10 °C between parameters is foreseen, and the temperatures of 200 and 210 °C were used as printing temperatures. The printing speeds were the optimum printing speeds predicted for these polymers in the software of the 3D printer used (3600 mm/min for PLA, 1500 mm/min for TPU) and the speeds obtained by reducing such optimum speed by 1/3 (2400 mm/min for PLA, 1000 mm/min for TPU). The infill rate was 100%, the infill geometry was rectilinear, and the layer thickness was 0.4 mm.

## Tensile Test

Tensile tests of both the samples attained by the injection method and the samples printed with a 3D printer were carried out with a Shimadzu (Shimadzu, Kyoto, Japan) universal testing device. The tensile speed was 5 mm/min for PLA matrices composites and 50 mm/min for TPU matrices composites.

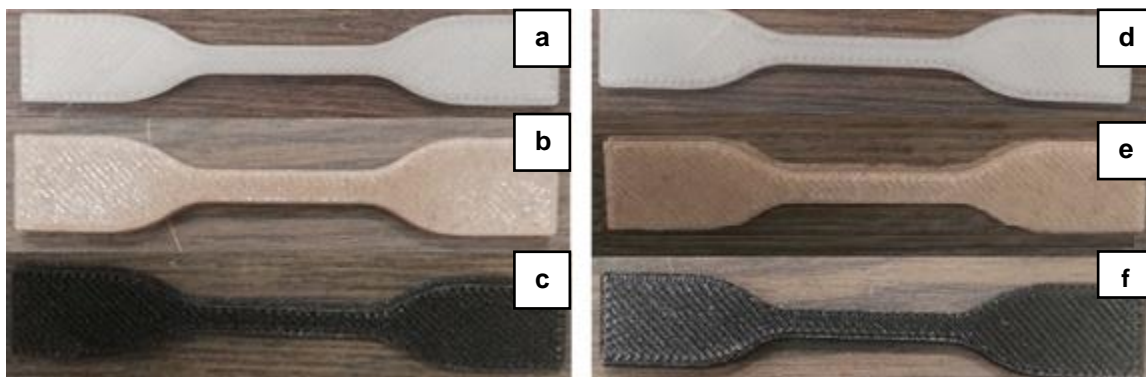


**Fig. 3.** 3D printed tensile test samples: (a) Pure PLA, (b) PLA-ARB, (c) PLA-L, (d) Pure TPU, (e) TPU-ARB, and (f) TPU-L

## Material Characterization

Scanning electron microscope (SEM) images of the printed samples were visualized with the TESCAN/MAIA3 XMU (Tescan Orsay Holding, a.s., Brno-Kohoutovice, Czech Republic) scanning electron microscope. The samples were gold plated with a Quorum 150T ES (Quorum Technologies Limited, Sussex, UK) instrument prior to examination.

## Thermal Analyses

Thermogravimetric analysis (TGA) and differential thermogravimetric analysis (DTG) of the test samples were performed with a Mettler Toledo TGA/DSC 1 HT (Mettler Toledo, Giessen, Germany) thermal analyzer in the temperature range of 25 to 1000 °C, heating rate of 10 °C/min, and nitrogen gas flow of 50 mL/min. Differential scanning calorimetry (DSC) analysis was performed with a Mettler Toledo DSC 1/700 (Mettler Toledo, Giessen, Germany) thermal analyzer in the temperature range of 0 °C to 600 °C and in a nitrogen medium.

## RESULTS AND DISCUSSION

### Thermal Analysis

The DSC thermograms (Fig. 4a) of pure PLA and PLA matrices composites demonstrate that ARB and L additives did not affect the glass transition temperature ( $T_g$ ), and they all had a single glass transition temperature (67 °C). A similar result was obtained by Gkartzou *et al.* (2017), and it was stated that this may be due to the low lignin contribution level and its  $T_g$  possibly overlapping with the melting peaks of PLA. Melting temperatures ( $T_m$ ) of pure PLA, PLA-L, and PLA-ARB composites were determined as 162, 155, and 163 °C, respectively. It can be said that the L additive reduced the melting

temperature of PLA by a small amount (7 °C), while the ARB additive did not change it. The melting ( $T_m$ ) values of pure TPU, TPU-ARB, and TPU-L composites were determined as 126, 165, and 115 °C, respectively. The addition of ARB increased the melting temperature of TPU. ARB, known as liquid wood, contains lignin (30 to 60%), natural reinforcing fibers (10 to 60%), and impact modifiers and fire retardants (approx. 10%) (Nedelcu *et al.* 2016). Such components composing the ARB increase thermal resistance.

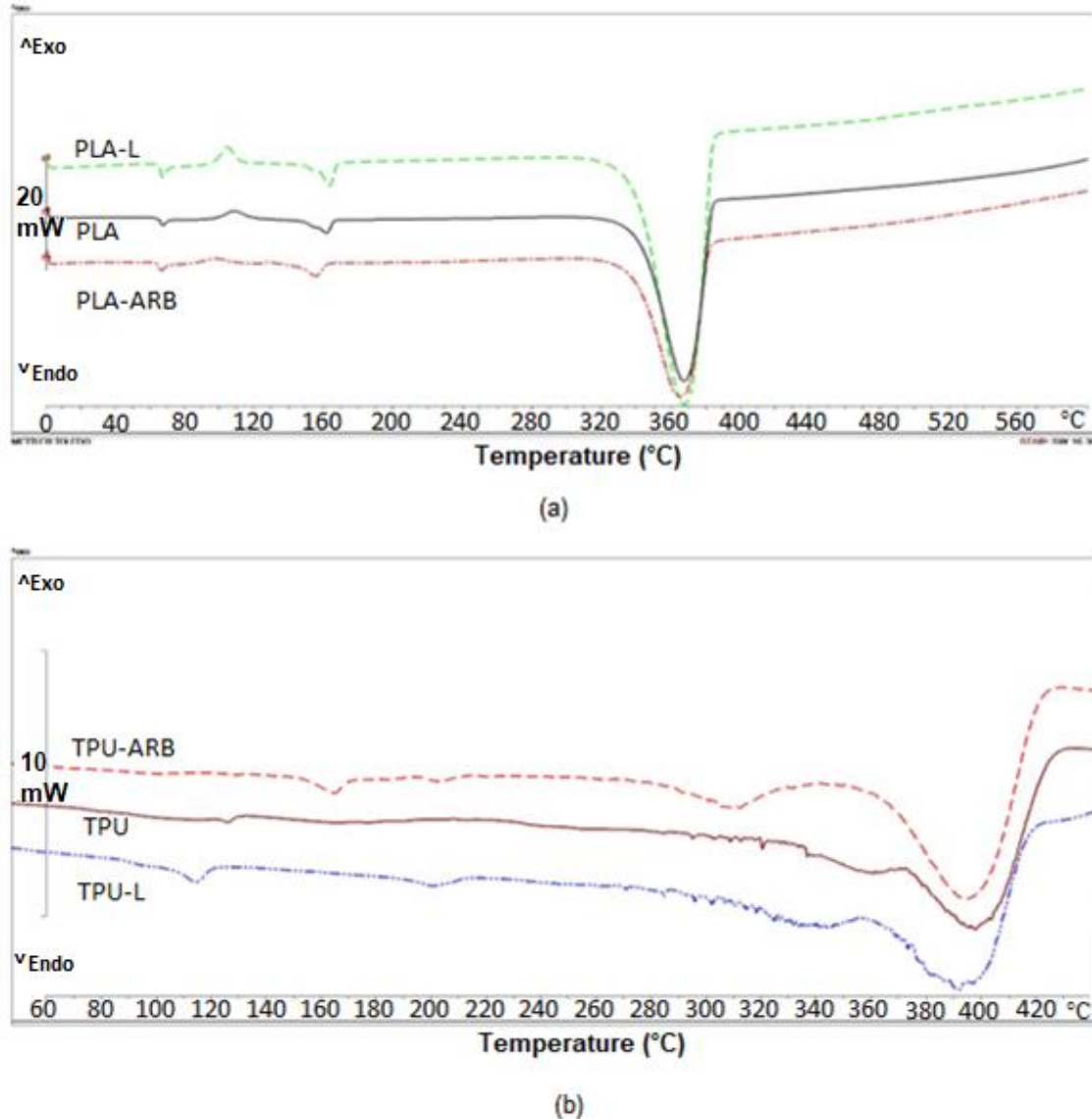
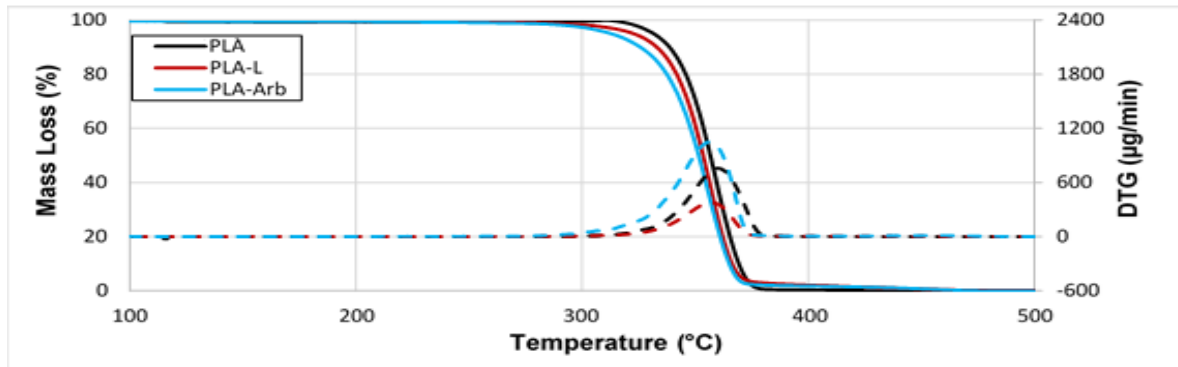


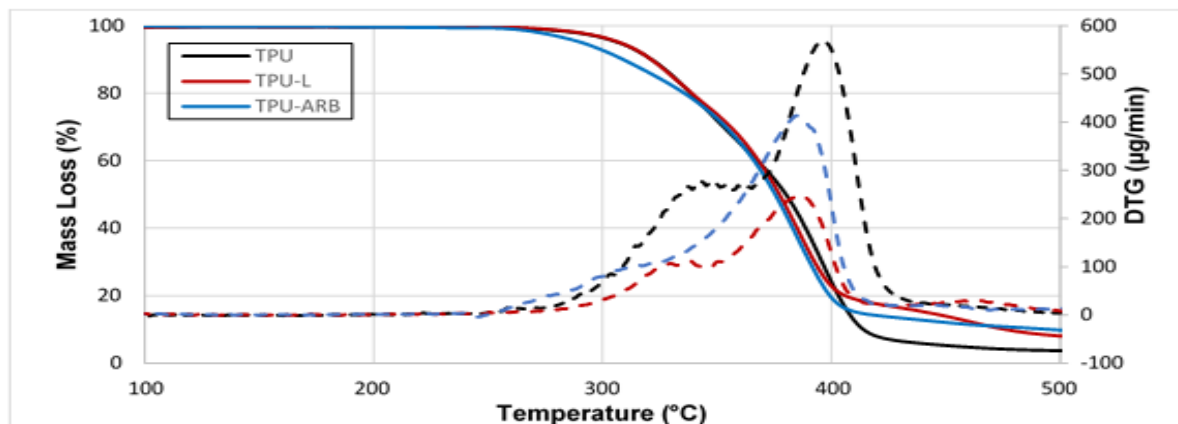
**Fig. 4.** DSC analysis results: (a) Composites with PLA matrix, (b) Composites with TPU matrix

The TGA data shows the weight loss due to temperature increase, and the first derivative (DTG) shows the corresponding weight loss ratio (Gkartzou *et al.* 2017). PLA, PLA-L, and PLA-ARB exhibited similar thermal degradation behavior (Fig. 5). It was observed that pure PLA started to decompose at 335 °C, whereas PLA-L and PLA-ARB started to decompose at 315 and 318 °C, respectively. Pure TPU started to degrade at 308 °C, TPU-L at 290 °C, and TPU-ARB at 289 °C. Such values of the TPU are consistent with

the study of Floros *et al.* (2012). Lignin and ARB additives reduced degradation temperatures in comparison to pure PLA and pure TPU. At 380 °C, 99% by mass of pure PLA, PLA-L and PLA-ARB composites had decomposed. Pure TPU, TPU-L, and TPU-ARB composites decomposed more than 90% by mass only at 500 °C. Gkartzou *et al.* (2017) and Tanase-Opedal *et al.* (2019) shared similar thermal results in their studies. Although L and ARB additives resulted in slight changes on the thermal degradation of PLA and TPU, such changes are not expected to have a remarkable negative impact on the filament production process as they occur well above the melting temperatures.



(a)



(b)

**Fig. 5.** TGA/DTG analysis results: (a) Composites with PLA matrix, (b) composites with TPU matrix

### Tensile Strength

Tensile tests were conducted with both injection molded and 3D printed samples. The mean and standard deviation values of the ultimate tensile strength and elongation at break are given in Table 2.

In the ultimate tensile strength (UTS) values of the samples attained by injection molding, L caused a decrease of about 15% and ARB by about 34% compared to pure PLA. The L and ARB additives were observed to have caused a decrease of 44% and 49%, respectively, in elongation at break values. In TPU matrices samples, on the other hand, the UTS value decreased 55% in L and 18% in ARB; elongation at break value decreased by 78% in L and 37% in ARB.

**Table 2.** The Ultimate Tensile Strength and Elongation at Break Values of Samples Attained by Injection and 3D Printing Processes

Material	Temperature (°C)	Print speed (mm/min)	Ultimate Tensile Strength (N/mm <sup>2</sup> )	Elongation at Break (%)
PLA	180	Injection Molded	64.93±2.27	9.13±1.413
	200	2400	61.85±1.64	6.18±0.381
		3600	54.69±1.46	5.09±0.419
	210	2400	49.95±1.00	8.34±0.289
		3600	42.71±1.33	4.62±1.368
	PLA-L	180	Injection Molded	54.74±1.82
200		2400	50.28±1.76	4.91±1.34
		3600	38.02±1.37	4.68±1.47
210		2400	37.57±2.22	4.24±1.18
		3600	35.22±2.61	3.93±0.397
PLA-ARB		180	Injection Molded	42.62±2.27
	200	2400	42.06±2.28	5.15±1.262
		3600	41.54±2.40	4.81±0.285
	210	2400	39.78±1.74	5.91±1.491
		3600	39.19±2.12	5.82±0.434
	TPU	180	Injection Molded	17.45±0.26
200		1000	14.39±0.24	1668±67
		1500	14.32±0.25	1424±85
210		1000	11.78±0.74	1254±92
		1500	8.59±0.77	1321±116
TPU-L		180	Injection Molded	7.93±0.29
	200	1000	5.08±0.14	330±74
		1500	4.62±0.29	371±41
	210	1000	4.56±0.21	337±66
		1500	3.97±0.28	270±17
	TPU-ARB	180	Injection Molded	14.35±0.20
200		1000	13.74±0.32	950±108
		1500	13.22±0.61	993±49
210		1000	12.96±0.24	940±25
		1500	11.33±0.69	859±49

The lignin is reported to induce an increase in hardness in composites due to its hard phenolic and aromatic texture, and generally to cause a brittle structure in composites, as it is a very low molecular weight (~3000 Da) solid additive (Nguyen *et al.* 2018). The mechanical and physical characteristics of the mixture are reported to be greatly affected by lignin-lignin, matrix-matrix, and matrix-lignin interactions and the immiscibility observed between the two components that constitute the composite is also stated to cause the brittleness of the composite to increase due to the low level of stress transfer between the lignin aggregates and the matrix (Gkartzou *et al.* 2017). It can be said that there is a

relatively better interfacial interaction between PLA and L and TPU and ARB additives. In the study of Bi *et al.* (2019), the tensile strength of 30% wood flour added TPU bio composite was reported as 18.16 MPa. Although the stated value is higher than the tensile strength of TPU-ARB (14.35 MPa) obtained in this study, it should be noted in terms of comparison that wood flour had been used in the cited study and more importantly, modifiers such as diphenylmethyl propane diisocyanate (MDI) and EPDM-g-MAH had been used to increase the interfacial interaction with TPU, and that such materials significantly increased the interfacial bonding between wood flour and TPU.

As expected, the UTS and elongation at break values of the PLA matrix samples printed with a 3D printer showed a slight decrease compared to the injected samples, but they were similar in terms of particular parameters. In the 3D printed samples, the UTS values changed inversely with the temperature and printing speed, so the highest values were achieved with the samples printed at 200 °C and 2400 mm/min speed. An increase in printing temperature of 10 °C resulted in average decreases of 20.5%, 16.5% and 5.5% in PLA, PLA-L, and PLA-ARB, respectively, and an increase in printing speed of 50% resulted in an average of 13%, 15% and 1.3% reductions in PLA, PLA-L and PLA-ARB, respectively. The highest changes were observed in L-added samples. Although interlayer adhesion is expected to increase with temperature increase, the temperature increase renders PLA prone to brittleness (Fernandes *et al.* 2018). In a similar study, Tanase-Opedal *et al.* (2019) reported higher UTS values for PLA+40% lignin samples printed at 215 °C compared to that of such printed at 230 °C. In the study examining the effect of printing temperature between 205 and 230 °C with 10% lignin added PLA filament, the optimum printing temperature was stated to be 215 °C (Gkartzou *et al.* 2017).

As expected, L and ARB additives slightly decreased elongation at break values for the samples printed with PLA matrix filaments. The printing parameters can be expressed to have no noticeable effect, despite being a little more evident in the samples printed at 210 °C. The low additive ratio and the already fragile structure of PLA have revealed such a result. The elongation at break values in all samples ranged between 3.9% and 6.2%.

The mechanical characteristics of the samples printed with TPU matrix filaments also decreased compared to the samples produced by injection. In the 3D-printed samples, the L addition remarkably (about 60%) lowered the UTS value, while the addition of ARB had much less effect. In fact, it was determined that there was an increase of about 30% in the samples printed at 210 °C and at a speed of 1500 mm/min. In terms of printing parameters, the increase in printing temperature and speed also induced a decrease in UTS and elongation at break values. The effect of a 10 °C print temperature increase on UTS was calculated as a reduction average of 29%, 12%, and 10% in TPU, TPU-L, and TPU-ARB, respectively. Increasing the printing speed, on the other hand, caused a decrease of approximately 14%, 11%, and 8% in TPU, TPU-L, and TPU-ARB samples, respectively. In samples printed with all three filaments, the highest UTS values were measured in samples printed with 200 °C temperature and 1000 mm/min print speed parameters. In the TPU-ARB composite, the tensile strength values of the injection molded samples and the printed samples were close to each other.

The stress-strain curves of the 3D-printed samples and the injection molded samples are given in Fig. 6. Since the printed samples displayed similar curves in their groups, only the data with the highest tensile strength values were used in the graph. It was observed that both L and ARB additions induced a decrease in strain values of the samples.

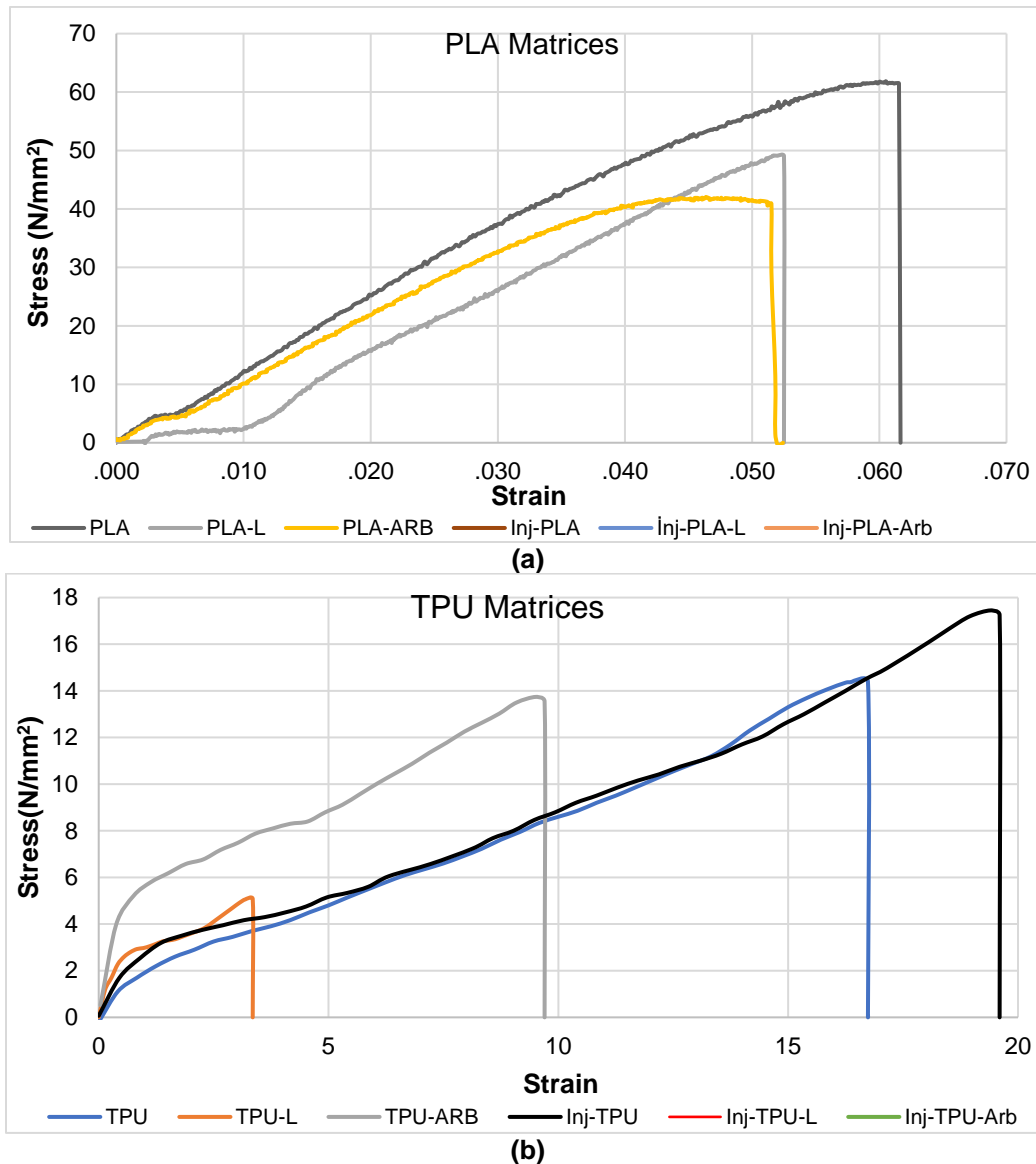


**Fig. 6.** (a) Stress-Strain curves of PLA matrix samples, (b) Stress-Strain curves of TPU matrix samples

Although the additives had similar effects on PLA, L had a very negative effect on both the elongation and tensile strength values of TPU. On the other hand, ARB did not decrease the ultimate tensile strength of TPU to a great extent in both injected and 3D printed samples, but on the contrary, it increased the tensile strength by approximately 40%, especially at low elongation values. It is possible to produce sufficiently strong flexible parts with the TPU-ARB filament. Upon examination of the mechanical characteristics of the 3D-printed parts, one should not focus on the maximum values obtained in the tests. This is because in the printed samples, the initial deformation occurs between the layers in the filling area, particularly in the TPU matrix ones, but the outer wall layers parallel to the tensile axis continue to exert strength. It is known that the tensile strength of samples printed in the longitudinal direction is higher than those printed in other directions, due to low adhesion between printing layers in samples produced with natural

fiber reinforced filaments (Le Duigou *et al.* 2016; Mazzanti *et al.* 2019). As the greatest shear stress under tensile stress occurs in the plane at an angle of 45 degrees to the tensile axis (Savaskan 2009), the partial decreases seen in the graph are induced by the filling geometry consisting of layers at an angle of 45 degrees to the drawing axis.

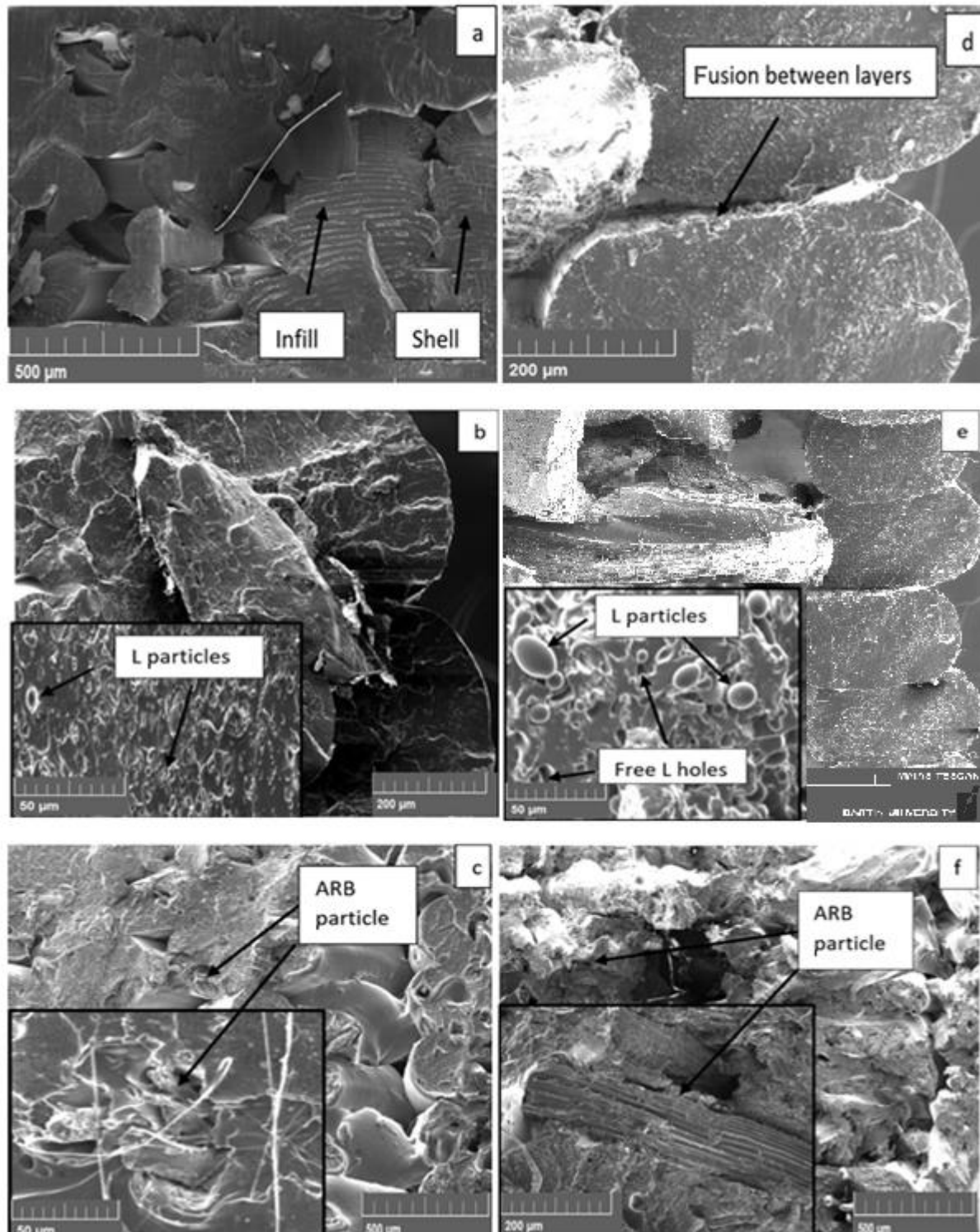


**Fig. 7.** (a) PLA, (b) PLA-L, (c) PLA-ARB, (d) TPU, (e) TPU-L, and (f) TPU-ARB

## Material Characterization

The fracture surfaces of the tensile test specimens printed using the printing parameters giving the best mechanical test results (200 °C and 2400 mm/min for PLA matrix specimens, 200 °C and 1000 mm/min for TPU) were investigated under SEM. The resulting micrographs give an idea regarding printing geometry and adhesion between layers (Fig. 7).

Upon examination of the micrographs of PLA and PLA matrix composites (Fig. 7a, b, c), the efficient execution of the adhesion between the filling geometry and the perimeter along with the interlayer adhesion can be observed. Mechanical test results also support such condition. The results are consistent with the literature (Gkartzou *et al.* 2017; Tanase-Opedal *et al.* 2019). Upon examination of the micrographs of TPU-ARB (Fig. 7f), the efficient execution of the adhesion between the filling geometry and the perimeter along with the interlayer adhesion can be observed. However, in accordance with the mechanical test results, there was partial achievement of adhesion between the filling geometry and the perimeter and the adhesion between the layers. In other words, inefficient adhesion can be observed in the TPU-L samples (Fig. 7e).

Although successful parts were produced by 3D printing using L and ARB added filaments in this study, it is possible to further increase both the adhesion between the additives and the main matrix and between the layers by using certain compatibilizing agents. There are compatibilizing agents in the literature for both PLA and TPU that are reported to increase interfacial bonding with additives. Among such, particularly the bio-based ones can be used to increase both L or ARB addition ratios and increase the mechanical characteristics of the resulting pieces. In order to determine the effect of such compatibilizing agents on the interlayer bonding during printing, further studies are planned by use of different printing parameters.

## CONCLUSIONS

1. Bio-based thermoplastic poly(lactic acid) (PLA) and bio-based thermoplastic polyurethane (TPU) were used as matrix, lignin and Arboform (ARB), which are also natural resources and wood-based materials, were used as additives, and a composite material was attained by successfully mixing with a twin-screw extruder. Some of the composites were processed by injection method, and some were obtained by extrusion method, and filament was attained for FDM 3D printers and parts were successfully printed.
2. According to the results of thermal analysis, lignin (L) and ARB additives decreased the thermal degradation temperatures of pure PLA and TPU, L additive decreased the melting temperature of PLA matrix slightly, whereas ARB additive induced an increase.
3. According to the mechanical test results; L and ARB additives induced a decrease in mechanical characteristics both in the samples obtained from the injection process and in the printed samples as expected. It was determined that particularly the L additive remarkably reduced the values in TPU matrix samples due to the weak TPU-L interfacial bond. It was possible to print parts having higher tensile strength with ARB added TPU filament compared to that of those produced with pure TPU filament.

4. The highest mechanical characteristic values were obtained at low printing speed and low printing temperatures in both TPU and PLA matrix samples. High printing temperature and speed caused a decrease in interlayer adhesion.
5. In the samples with PLA matrix, both the interlayer adhesion and the adhesion between the infill and the perimeter were achieved sufficiently. It was determined that the adhesion between the layers was weak, particularly in the samples printed with TPU-L filament.
6. It was determined that it is possible to produce pieces comparable to those produced by injection in 3D printers, using both PLA and TPU matrix composite filaments. The performance of the pieces can be increased by optimizing printing parameters by conducting more extensive studies on such parameters.

## ACKNOWLEDGMENTS

The authors are grateful to Professor Dr. Deniz Aydemir and Associate Professor Dr. Hüseyin Yörür for support in thermal analysis and expert feedback. The authors are grateful for the support of the Karabuk University Scientific Research Project Coordination Office under Grant No. KBUBAP-17-DR-407.

## REFERENCES CITED

- Arboform LV4 (2021). “TECNARO – The biopolymer company,” Tecnar (https://www.tecnaro.de/en/arboblend-arbofill-arboform/), Accessed 18 Oct 2021.
- Bates, S. R. G., Farrow, I. R., and Trask, R. S. (2016). “3D printed polyurethane honeycombs for repeated tailored energy absorption,” *Materials and Design*. DOI: 10.1016/j.matdes.2016.08.062
- Bi, H.-J., Ren, Z.-C., Guo, R., Xu, M., and Song, Y. (2018). “Fabrication of flexible wood flour/thermoplastic polyurethane elastomer composites using fused deposition molding,” *Industrial Crops and Products* 122, 76-84. DOI: 10.1016/j.indcrop.2018.05.059
- Dehne, L., Vila Babarro, C., Saake, B., and Schwarz, K. U. (2016). “Influence of lignin source and esterification on properties of lignin-polyethylene blends,” *Industrial Crops and Products* 86, 320-328. DOI: 10.1016/j.indcrop.2016.04.005
- Le Duigou, A., Castro, M., Bevan, R., and Martin, N. (2016). “3D printing of wood fibre biocomposites: From mechanical to actuation functionality,” *Materials and Design* DOI: 10.1016/j.matdes.2016.02.018
- Fernandes, J., Deus, A. M., Reis, L., Vaz, M. F., and Leite, M. (2018). “Study of the influence of 3D printing parameters on the mechanical properties of PLA,” *Proceedings of the International Conference on Progress in Additive Manufacturing*, 2018-May, pp. 547-552. DOI: 10.25341/D4988C
- Floros, M., Hojabri, L., Abraham, E., Jose, J., Thomas, S., Pothan, L., Leao, A. L., and Narine, S. (2012). “Enhancement of thermal stability, strength and extensibility of

- lipid-based polyurethanes with cellulose-based nanofibers,” *Polymer Degradation and Stability* 97(10), 1970-1978. DOI: 10.1016/j.polymdegradstab.2012.02.016
- Gkartzou, E., Koumoulos, E. P., and Charitidis, C. A. (2017). “Production and 3D printing processing of bio-based thermoplastic filament,” *Manufacturing Review* 4. DOI: 10.1051/mfreview/2016020
- Gordobil, O., Delucis, R., Egüés, I., and Labidi, J. (2015). “Kraft lignin as filler in PLA to improve ductility and thermal properties,” *Industrial Crops and Products* 72, 46-53. DOI: 10.1016/j.indcrop.2015.01.055
- Kariz, M., Sernek, M., Obućina, M., and Kuzman, M. K. (2018). “Effect of wood content in FDM filament on properties of 3D printed parts,” *Materials Today Communications* 14, 135-140. DOI: 10.1016/j.mtcomm.2017.12.016
- Lee, J. S., Hong, J. M., Jung, J. W., Shim, J. H., Oh, J. H., and Cho, D. W. (2014). “3D printing of composite tissue with complex shape applied to ear regeneration,” *Biofabrication* 6(2). DOI: 10.1088/1758-5082/6/2/024103
- Li, H., Liang, Y., Li, P., and He, C. (2020). “Conversion of biomass lignin to high-value polyurethane: A review,” *Journal of Bioresources and Bioproducts* 5(3), 163-179. DOI: 10.1016/j.jobab.2020.07.002
- Liu, L., Lin, M., Xu, Z., and Lin, M. (2019). “Polylactic acid-based wood-plastic 3D printing composite and its properties,” *BioResources* 14(4), 8484-8498. DOI: 10.15376/biores.14.4.8484-8498
- Mazzanti, V., Malagutti, L., and Mollica, F. (2019). “FDM 3D printing of polymers containing natural fillers: A review of their mechanical properties,” *Polymers* 11(7). DOI: 10.3390/polym11071094
- Mimini, V., Sykacek, E., Hashim, S. N. A., Holzweber, J., Hettegger, H., Fackler, K., Potthast, A., Mundigler, N., and Rosenau, T. (2019). “Compatibility of kraft lignin, organosolv lignin and lignosulfonate with PLA in 3D printing,” *Journal of Wood Chemistry and Technology* 39(1), 14-30. DOI: 10.1080/02773813.2018.1488875
- Nedelcu, D., Lohan, N. M., Volf, I., and Comaneci, R. (2016). “Thermal behaviour and stability of the Arboform® LV3 nature liquid wood,” *Composites Part B: Engineering* 103, 84-89. DOI: 10.1016/j.compositesb.2016.08.023
- Nguyen, N. A., Bowland, C. C., and Naskar, A. K. (2018). “A general method to improve 3D-printability and inter-layer adhesion in lignin-based composites,” *Applied Materials Today* 12, 138-152. DOI: 10.1016/j.apmt.2018.03.009
- Raj, S. A., Muthukumar, E., and Jayakrishna, K. (2018). “A case study of 3D printed PLA and its mechanical properties,” *Materials Today: Proceedings* 5(5), 11219-11226. DOI: 10.1016/j.matpr.2018.01.146
- Savaşkan, T. (2009). *Malzeme Bilgisi ve Muayenesi*, Celepler Matbaacılık, Trabzon, Türkiye. ISBN:978-9944-0068-1-1
- Solihat, N. N., Sari, F. P., Falah, F., Ismayati, M., Lubis, M. A. R., Fatriasari, W., Santoso, E. B., and Syafii, W. (2021). “Lignin as an active biomaterial: A review,” *Jurnal Sylva Lestari* 9(1), 1. DOI: 10.23960/jsl191-22
- Spiridon, I., Leluk, K., Resmerita, A. M., and Darie, R. N. (2015). “Evaluation of PLA-lignin bioplastics properties before and after accelerated weathering,” *Composites Part B: Engineering* 69, 342-349. DOI: 10.1016/j.compositesb.2014.10.006

- Spiridon, I., and Tanase, C. E. (2018). "Design, characterization and preliminary biological evaluation of new lignin-PLA biocomposites," *International Journal of Biological Macromolecules* 114, 855-863. DOI: 10.1016/j.ijbiomac.2018.03.140
- Tanase-Opedal, M., Espinosa, E., Rodríguez, A., and Chinga-Carrasco, G. (2019). "Lignin: A biopolymer from forestry biomass for biocomposites and 3D printing," *Materials* 12(18), 1-15. DOI: 10.3390/ma12183006
- Wimmer, R., Steyrer, B., Koddenberg, T., and Mundigler, N. (2015). "3D printing and wood," *Pro-Ligno* 11(4), 144-149.

Article submitted: March 1, 2021; Peer review completed: May 8, 2021; Revised version received and accepted: October 29, 2021; Published: November 3, 2021.  
DOI: 10.15376/biores.17.1.21-36